Electronic Supplementary Material (ESI) for Lab on a Chip.

Supplementary Information

Robust fully controlled nanometer liquid layers for high resolution liquid-cell electron microscopy

Tyler S. Lott[1†], Ariel A. Petruk[1†], Nicolette A. Shaw[1], Natalie Hamada[2], Carmen M. Andrei[2], Yibo Liu[3], Juewen Liu[3], and Germán Sciaini[1*]

1. The Ultrafast electron Imaging Laboratory (UeIL), Department of Chemistry and Waterloo Institute for Nanotechnology (WIN), University of Waterloo, 200 University Ave. W., N2L 3G1, Waterloo, Ontario, Canada

2. The Canadian Centre for Electron Microscopy, McMaster University, A.N. Bourns Science Building, 1280 Main St. W., L8S 4M1, Hamilton, Ontario, Canada

3. Department of Chemistry and Waterloo Institute for Nanotechnology (WIN), University of Waterloo, 200 University Ave. W., N2L 3G1, Waterloo, Ontario, Canada.

[†]Equal contributions

[*]Correspondence: gsciaini@uwaterloo.ca

Supplementary Note 1: Infrastructure

Transmission electron microscopy

Liquid-cell transmission electron microscopy (LC-TEM) experiments were performed at the Canadian Centre for Electron Microscopy (CCEM) utilizing two main transmission electron microscopes (TEMs), a Talos 200X and a Titan HB.

CCEM's Talos 200X has an X-FEG (Schottky type) high-brightness field emission gun, which was operated at 200 kV. It is equipped with a CETA 16M CMOS camera and a GIF Continuum S Gatan system with a low-noise and high dynamic range CMOS detector.

CCEM's Titan HB has an X-FEG electron gun, UltiMono monochromator, probe and image aberration correctors (CEOS). This TEM was operated at 300 kV, and it was equipped with an Ultrascan CCD camera (Gatan) and a GIF Quantum (Gatan). This tool has been decommissioned and it is being replaced by a new Thermo-Fisher Spectra Ultra.

LC-TEM Kit

The LC-TEM kit is proprietary technology that has been developed at UeIL to suit Thermo-Fisher TEMs. Holders and loading stations were machined at the Faculty of Science Machining Services Shop. Nanofluidic cells (NFCs) were produced in house at the University of Waterloo Quantum Nano-Fabrication Core Facility (QNFCF).

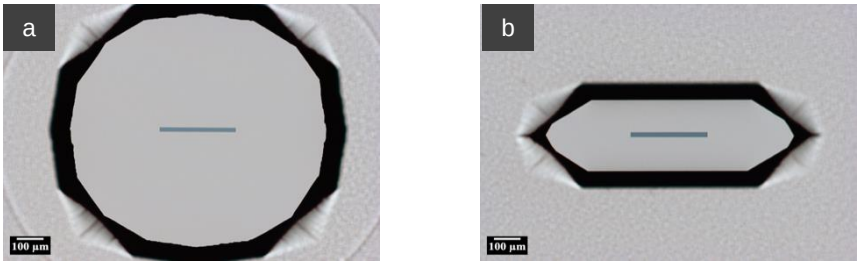

Fig. S1: Optical microscope images of the nanofluidic cell surfaces. a. Central pillar of the bottom NFC chip. **b.** Central pillar of the top NFC chip.

NFCs were produced with defined spacers of approximately 100 nm, 200 nm, 550 nm, and 630 nm. During the assembly process a top NFC chip and a bottom NFC chip are brought together to ensure a cross-over with the length of one window and the width of the other. Due to the tolerances in machining, such an assembly process ensures that the two NFC windows are

always overlapped when the nanofluidic cell assembly is formed. The silicon nitride (SiN_x) windows have dimensions of ≈ 20 µm x 300 µm and a thickness of 30 nm. Images of the bottom NFC chip (left) and top NFC chip (right) pillars are shown in Figure S1.

Supplementary Note 2: Materials and Methods

Gold (Au) nanorods: 1 OD (optical density) nanoXact monodisperse Au nanorods (40 nm x 15 nm, sodium citrate capping agent) dispersed in United States Pharmacopeia (USP) grade purified water were purchased from nanoComposix Inc. (San Diego, CA) and were used as prepared without dilution. Approximately 400 nL (nominal) of this solution was dispensed onto the surface of the bottom NFC. The sample was then sealed within the nanofluidic cell assembly using the method described herein.

Polystyrene (PS) nanospheres: 10 mg mL^{-1} colloidal PS nanospheres (100 nm diameter, non-functionalized surface) dispersed in Milli-Q water were purchased from ALPHA Nanotech (Vancouver, B.C.) and were diluted prior to imaging (1:25) in 18.2 MΩ-cm ultra-purified water. This solution was aspirated with a micropipette before sample delivery. Approximately 400 nL (nominal) of this solution was dispensed onto the surface of the bottom NFC. The sample was then sealed within the nanofluidic cell assembly using the method described herein.

DOPC Liposomes: DOPC (1,2-dioleoyl-sn-glycero-3-phosphocholine) phospholipid was purchased from Avanti Polar Lipids (Alabaster, AL). 4-(2-hydroxyethyl)-1-piperazineethanesulfonic acid (HEPES) was purchased from Sigma-Aldrich. Sodium chloride was purchased from Mandel Scientific (Guelph, ON). Milli-Q water was used to prepare all samples.

DOPC liposomes were prepared using the standard extrusion method. DOPC lipid (2.5 mg) was dissolved in chloroform (100 µL). After evaporating chloroform by gently blowing with N_2 to form a thin film, the film was dried in a vacuum oven at room temperature overnight to fully remove residual chloroform. The dried lipid film was stored at -20 °C in a nitrogen atmosphere prior to use. To prepare liposomes, the lipid films were hydrated with 0.5 mL buffer (10 mM HEPES, pH 7.6, with 100 mM NaCl) yielding a lipid concentration of 5 mg mL^{-1}. The resulting cloudy suspension was extruded 21 times through two stacked polycarbonate membranes with a pore size of 100 nm to yield a clear liposome suspension. Approximately

400 nL (nominal) of this solution was dispensed onto the surface of the bottom NFC. The sample was then sealed within the nanofluidic cell assembly using the method described herein.

Surface treatment of NFCs

For all experiments, the surface of the top NFC was preconditioned in a H_2/Ne/Ar plasma (Gatan Solarus Model 950 Advanced Plasma System) at 30 W for 2 minutes.

Supplementary Note 3: Membrane Deformation Measurements

We performed window deformation measurements as a function of gas pressure differential (ΔP) and window width (W) across a SiN_x membrane with a thickness of 25 nm. These measurements provide upper limit estimates because they neglect the adhesive and cohesive forces of the liquid phase. H corresponds to the maximum deformation measured at the centre of the membrane. More details can be found elsewhere.[1]

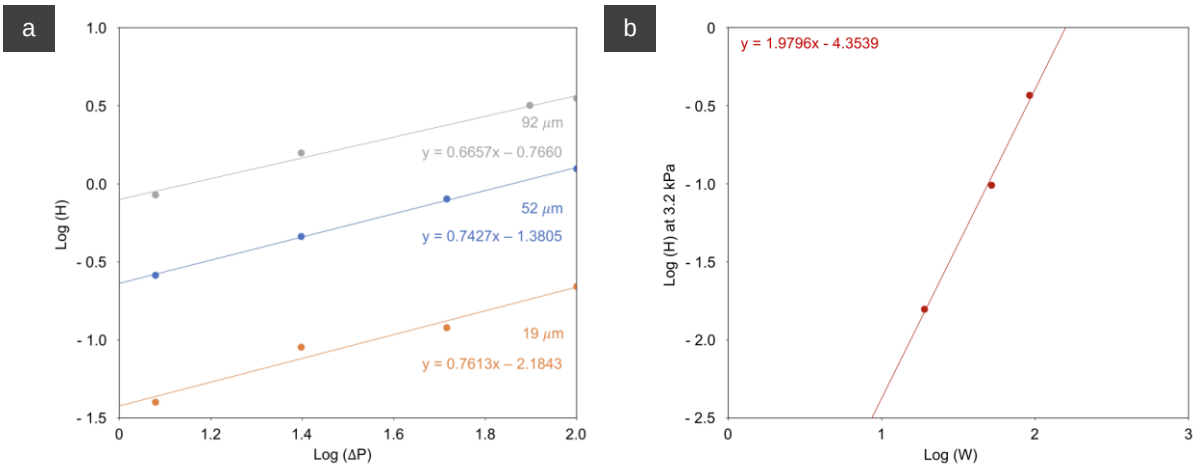

Fig. S2: Window deformation measurements for a 25-nm thick SiN_x membrane. **a.** Log_{10} of the pressure differential (ΔP) in kPa versus log_{10} of the maximum deformation (H) in microns for windows with widths (W) of 92 µm (grey trace), 52 µm (blue trace), and 19 µm (orange trace). **b.** Log_{10}(W) versus log_{10}(H) for $\Delta P = 3.2$ kPa (the vapour pressure of pure water at 25°C).

Supplementary Note 4: Liquid Layer Characterization

Electron energy loss spectroscopy (EELS) was conducted on both the Talos 200X and the FEI Titan HB. In the former, the collection angle of the EELS spectrometer was set to 23 mrad

while in the latter the collection angle was set to 55 mrad. Data were collected through Gatan Digital Micrograph and later exported for analysis using Hyperspy and custom Python scripts.

The liquid layer thickness was determined through the log-ratio method by Egerton and co-workers (Eq. S1)[2,3]:

$$\frac{t}{\lambda} = \ln\left(\frac{I}{I_0}\right) \tag{S1}$$

where I is the total number of electrons in the EELS spectrum (e.g., 'yellow plus pink' areas in Fig. S3b) and I_0 is the number of electrons having lost no energy (the zero-loss peak, e.g., yellow area in Fig. S3b), t is the thickness of specimen, and λ is the inelastic mean free path of the electrons as outlined in Eq. S2:

$$\lambda \approx \frac{106FE_0}{E_m \ln\left(\frac{2\beta E_0}{E_m}\right)} \tag{S2}$$

where E_0 is the electron energy in keV, β is the collection angle of the EELS spectrometer in mrad, F is a relativistic factor, and E_m is the average energy loss in eV, which has been estimated as shown in Eq. S3[2,3]:

$$E_m = 7.6Z_{eff}^{0.36} \tag{S3}$$

Z_{eff} is the effective atomic number of the material which is being investigated.[2,3] For the purposes of this paper, we calculate the Z_{eff} using the Lenz model[3,4]:

$$Z_{eff} = \frac{\sum_i f_i Z_i^{1.3}}{\sum_i f_i Z_i^{0.3}} \tag{S4}$$

where f_i is the atomic fraction and Z_i is the atomic number.

Quantification of the liquid layer thickness in an NFC necessitates the collection of two EELS spectra. One EELS spectrum of the nanofluidic cell in the absence of liquid and one EELS spectrum of the nanofluidic cell in the presence of liquid between the two window membranes. This data collection will allow one to perform a background subtraction of the silicon nitride contribution to the EELS spectrum of the assembled nanofluidic cell:

$$\frac{t_{total}}{\lambda_{total}} = \frac{t_w}{\lambda_w} + \frac{t_{SiN_x}}{\lambda_{SiN_x}} \tag{S5}$$

Where t_{total} is the total thickness, λ_{total} is the total inelastic mean free path, t_w and t_{SiN_x} are the thicknesses of the water layer and the SiN_x membranes, respectively; and λ_w and λ_{SiN_x} are the electron inelastic mean free paths in water and SiN_x, respectively.

From Eq. S1 and Eq. S5, we obtain,

$$t_w = \left(\ln\left(\frac{I}{I_0}\right)_{total} - \ln\left(\frac{I}{I_0}\right)_{SiN_x} \right) \times \lambda_w \tag{S6}$$

Where the subscripts '$total$' refers to the full NFC with pure water and 'SiN_x' refers to an empty NFC. Note that $\ln\left(\frac{I}{I_0}\right)_{total}$ and $\ln\left(\frac{I}{I_0}\right)_{SiN_x}$ are determined experimentally under the same conditions and λ_w is calculated via Eqs. S2 – S4. We obtained the values of λ_w = 154 nm and 161 nm for the EELS experimental conditions in the Talos 200X and Titan HB, respectively. However, it should be mentioned that these values of λ_w may be underestimated by about 50% as recently indicated by Yesibolati et al..[6]

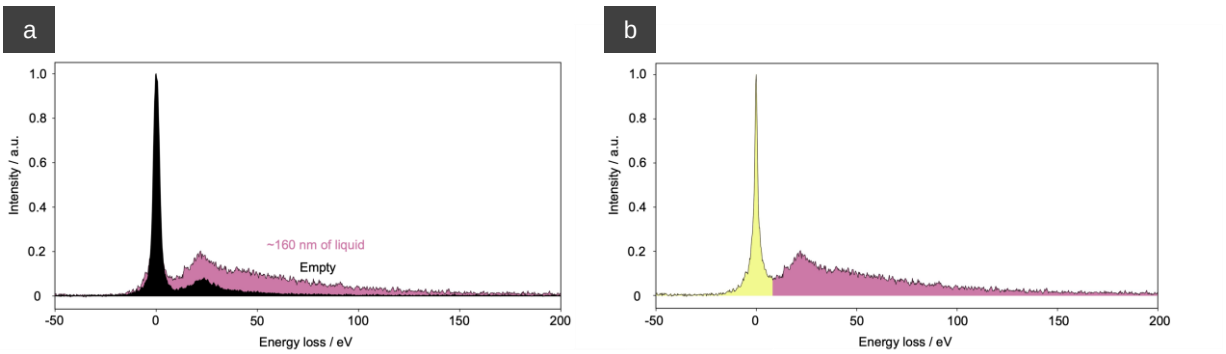

Fig. S3: Raw EELS spectra. a. EELS spectra obtained in a Titan HB showing the intensity differences between a nanofluidic cell with a liquid layer thickness of ≈ 160 nm (pink) and an empty (black) nanofluidic cell. **b.** The liquid layer thickness was determined using the log-ratio method where the zero-loss peak (ZLP) and spectrum areas were calculated using Simpson's method. The ZLP area was determined by integrating the signal up to the valley as indicated by the yellow area in **b**. Similar results were obtained by fitting the ZLP with a Gaussian function.

EELS measurements were conducted as line scans to illustrate the high degree of uniformity present in the silicon nitride membranes. The accumulation of carbon contamination during STEM-EELS measurements is a known challenge within the electron microscopy community.

To avoid the influence of carbon contamination during the course of the EELS line scan, in addition to plasma cleaning of the nanofluidic cells and the sample holder, the region of interest was found using a defocused STEM probe (~ 100 µm of defocus). An electron micrograph illustrating a typical line scan region used for thickness measurements is shown in Fig. S4. Control experiments were done and showed that this amount of defocus does not alter the EELS spectrum but largely reduced the carbon contamination.

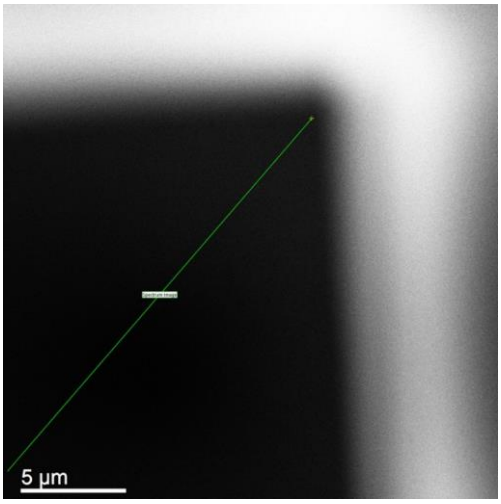

Fig. S4: High-angle annular dark field image showing a representative line scan region. The green line denotes the path of the EELS line scan carried out with the same defocus to avoid carbon deposition.

Supplementary Note 5: Electron Beam Transmission Estimation

Electron transmission can be calculated using total elastic scattering cross-section data.[7] The data used was obtained by Riley et al.[7] and a Python program was written to perform the calculations below. The experimental total elastic scattering cross section, σ_{el} is converted to the total scattering cross section, σ_{tot} in Eq. S7 where Z is the atomic number.[6]

$$\sigma_{tot} = 18\,\sigma_{el}/Z\ +\ \sigma_{el} \tag{S7}$$

The total mean free path, Λ_{tot} is then calculated using Eq. S8, where the compound SiN_x with stoichiometric composition Si_3N_4 is shown as an example. In Eq. S8, N_j is the number density of the element, N_A is Avogadro's number, and ρ and M are the density and molecular weight of Si_3N_4, respectively.

$$\Lambda_{tot} = \frac{1}{\sum N_j \sigma_{tot,j}} = \frac{1}{N_{Si_3N_4}\left(3\,\sigma_{tot,Si} + 4\,\sigma_{tot,N}\right)} = \\ = \frac{1}{\frac{N_A\,\rho}{M}\left(3\,\sigma_{tot,Si} + 4\,\sigma_{tot,N}\right)} \tag{S8}$$

The relationship between the total mean free path and beam energy for different LC window materials and liquid water is shown in Fig. S5a. Amorphous carbon and graphene are both represented as carbon. Electron transmission is finally calculated using the total mean free path and thickness of the material using Eq. S9.

$$T = e^{-t/\Lambda_{tot}} \tag{S9}$$

Fig. S5b shows the thickness of liquid water needed to reach the same electron transmission as 10 nm SiN_x as a function of electron beam energy (where $\Lambda_{tot,liquid\ H_2O}$ is estimated as an average of $\Lambda_{tot,O}$ and Λ_{tot,He_2O} calculated with $N_{liquid\ water}$). In terms of loss in transmission, the plot shows that 10 nm SiN_x windows (5 nm each) corresponds to approximately 40 nm of water.

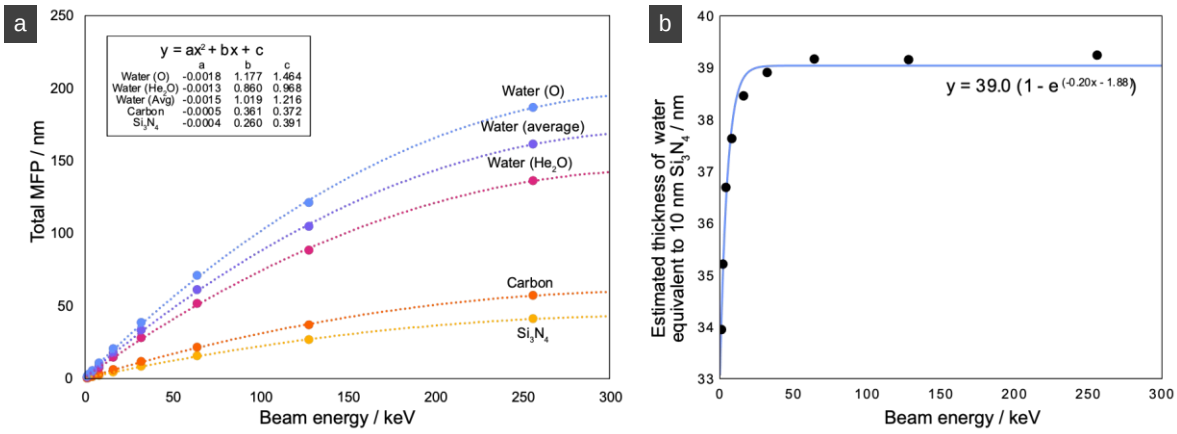

Fig. S5: Electron beam transmission estimation. a. Total electron mean free path as a function of the electron beam energy.[6,7] The inset shows the parameters for the second order polynomial fits for each trendline (dotted lines). The Water (O) data was calculated using experimental oxygen data (assuming no contribution of hydrogen), where Water (He_2O) was modelled with experimental helium data in the place of hydrogen data.[7] Both were calculated using the number density of water with a density of 1.0 g cm^{-3}. The density values of Carbon and Si_3N_4 were taken to be 2.0 g cm^{-3}, and 3.2 g cm^{-3} respectively.[6,8] **b.** Calculated thickness of water (average) equivalent in electron beam transmission to 10 nm SiN_x as a function of electron beam energy. The blue line and equation depict the trend of the data.

Supplementary Movies

Supplementary Movie 1: Illustration of the nanofluidic cell assembly process.

Supplementary Movie 2: Au nanorods imaged at 200 kV near the corner of the viewing area (ViA). Magnification = 74kx. Dose rate ≈ 15 electrons $Å^{-2}$ s^{-1}.

Supplementary Movie 3: Au nanorods imaged at 200 kV near the centre of ViA. Magnification = 94kx. Dose rate ≈ 25 electrons $Å^{-2}$ s^{-1}.

Supplementary Movie 4: Au nanorods imaged at 300 kV near the centre of ViA. Magnification = 450kx. Dose rate ≈ 7.0 x 10^3 electrons $Å^{-2}$ s^{-1}. We observe nanoparticle sintering and facet formation.

Supplementary Movie 5: Au nanorods imaged at 200 kV illustrating electron beam induced dendritic-like growth. Magnification = 244k. Dose rate ≈ 130 electrons $Å^{-2}$ s^{-1}.

Supplementary Movie 6: Au nanorods imaged at 200 kV illustrating the electron beam induced formation of bubbles under prolonged imaging conditions. Magnification = 224kx. Dose rate ≈ 130 electrons $Å^{-2}$ s^{-1}.

Supplementary Movie 7: DOPC liposomes imaged at 200 kV near the centre of ViA. Magnification = 22kx. Dose rate ≈ 1.5 electrons $Å^{-2}$ s^{-1}. We observed *unstained* liposomes with sufficient contrast and their beam induced structural degradation over the course of approximately one minute.

Supplementary Movie 8: Au nanorods imaged at 300 kV with high resolution near the centre of ViA. Magnification = 600kx. Dose rate ≈ 1.2 x 10^4 electrons $Å^{-2}$ s^{-1}. We observed lattice planes and nanoparticle growth.

References

1. Petruk, A. A., Allen, C., Rivas, N., Pichugin, K. & Sciaini, G. High flow rate nanofluidics for *in-liquid* electron microscopy and diffraction. *Nanotechnology* **30**, 395703 (2019).
2. Egerton, R. F. *Electron Energy-Loss Spectroscopy in the Electron Microscope*. (Springer US, 2011). doi:10.1007/978-1-4419-9583-4.

3. Malis, T., Cheng, S. C. & Egerton, R. F. EELS log-ratio technique for specimen-thickness measurement in the TEM. *J. Electron Microsc. Tech.* **8**, 193–200 (1988).
4. Lenz, F. Zur Streuung mittelschneller Elektronen in kleinste Winkel. *Z. Naturforsch. A* **9**, 185-204 (1954).
5. Yesibolati, M. N. *et al.* Electron inelastic mean free path in water. *Nanoscale* **12**, 20649–20657 (2020).
6. Dwyer, J. R. & Harb, M. Through a Window, Brightly: A Review of Selected Nanofabricated Thin-Film Platforms for Spectroscopy, Imaging, and Detection. *Appl. Spectrosc.* **71**, 2051–2075 (2017).
7. Riley, M. E., MacCallum, C. J. & Biggs, F. Theoretical electron-atom elastic scattering cross sections. *At. Data Nucl. Data Tables* **15**, 443–476 (1975).
8. Yen, B. K. *et al.* Microstructure and properties of ultrathin amorphous silicon nitride protective coating. *J. Vac. Sci. Technol. A* **21**, 1895–1904 (2003).